

Tuning Reaction and Diffusion Mediated Degradation of Enzyme-Sensitive Hydrogels

Stacey C. Skaalure, Umut Akalp, Franck J. Vernerey,* and Stephanie J. Bryant*

Supporting Information for this article is available as a supplementary PDF file, accessible from the article page on Wiley Online Library. For more information on this service please go to the journal web page on Wiley Online Library at www.interscience.wiley.com.
 The following text is a placeholder for the abstract and supporting information, which is mostly illegible in the provided image. It appears to contain technical details and references related to the hydrogel degradation study.

a crosslinked solid polymer (i.e., fluorescent regions) to a soluble polymer where the polymer chains rapidly diffuse out into the bath (i.e., nonfluorescent regions). This critical point is correlated to the degree of network connectivity during hydrogel formation (i.e., the gel point), which has been described for an ideal network using a statistical network formation model (Equation (S2), Supporting Information)^{9]} Experimentally, we observe a degradation front where the region of the hydrogel adjacent to the enzyme source is completely degraded, which advances along the length of the hydrogel, away from the

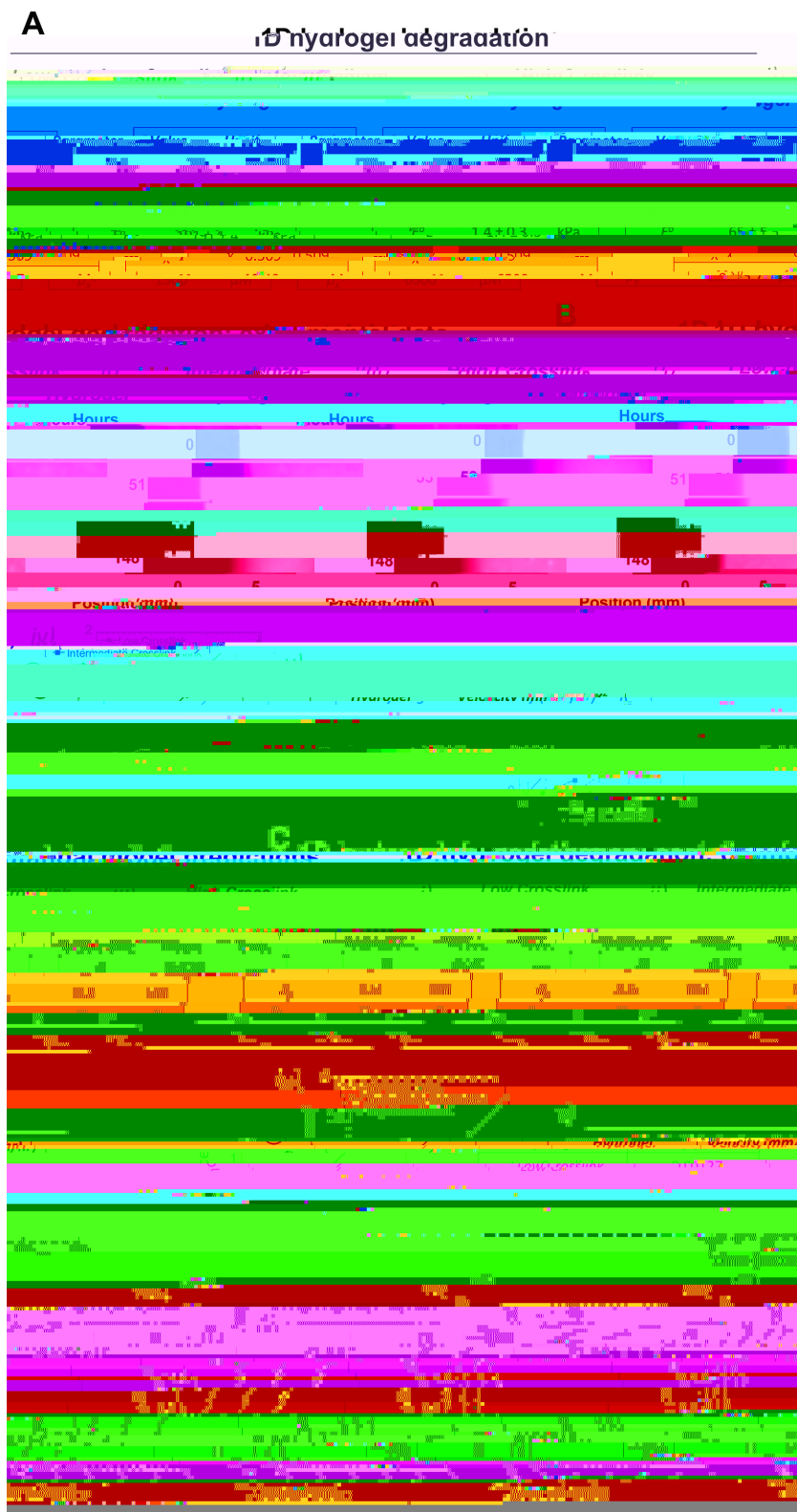


Figure 1. Spatiotemporal changes in crosslink density for three hydrogel cases: (A) intermediate crosslink, (B) low crosslink, and (C) high crosslink. The color scale represents crosslink density, with red indicating high density and blue indicating low density.

crosslinked hydrogel case, a wide front that propagates quickly is observed resulting in an overall decrease in the crosslink density of the bulk hydrogel for Pnite distances (e.g., at 5 mm) (Figure 1Cvi). In the intermediate and high crosslink hydrogel cases, a sharp front is observed and the initial bulk hydrogel properties are largely maintained (Figure 1Cvii,viii). We demonstrate that the model is able to capture the propagating front and front width, especially for the intermediate and high crosslink hydrogel cases (Figure S4, Supporting Information). However due to limitations in the experimental set-up, the fluorescence in the low crosslinked hydrogel does not directly correlate to crosslink density and therefore the front width could not be matched to the model (see Figure S4, Supporting Information). Nonetheless, the model can be used to describe the spatiotemporal changes in crosslink density for each of the three hydrogel cases.

We next extended the experimental and computational analysis to 3D, using a low and high crosslinked hydrogel with formulations given in Table S1 and initial properties in Figure 2A. Experimentally, we developed a cell-mimetic platform (Scheme 1C) using collagenase-loaded PLGA microparticles encapsulated in the enzyme-sensitive PEG hydrogel. Prior to encapsulation, release of collagenase from the microparticles was characterized by a rapid burst release followed by a slow yet sustained release of enzyme

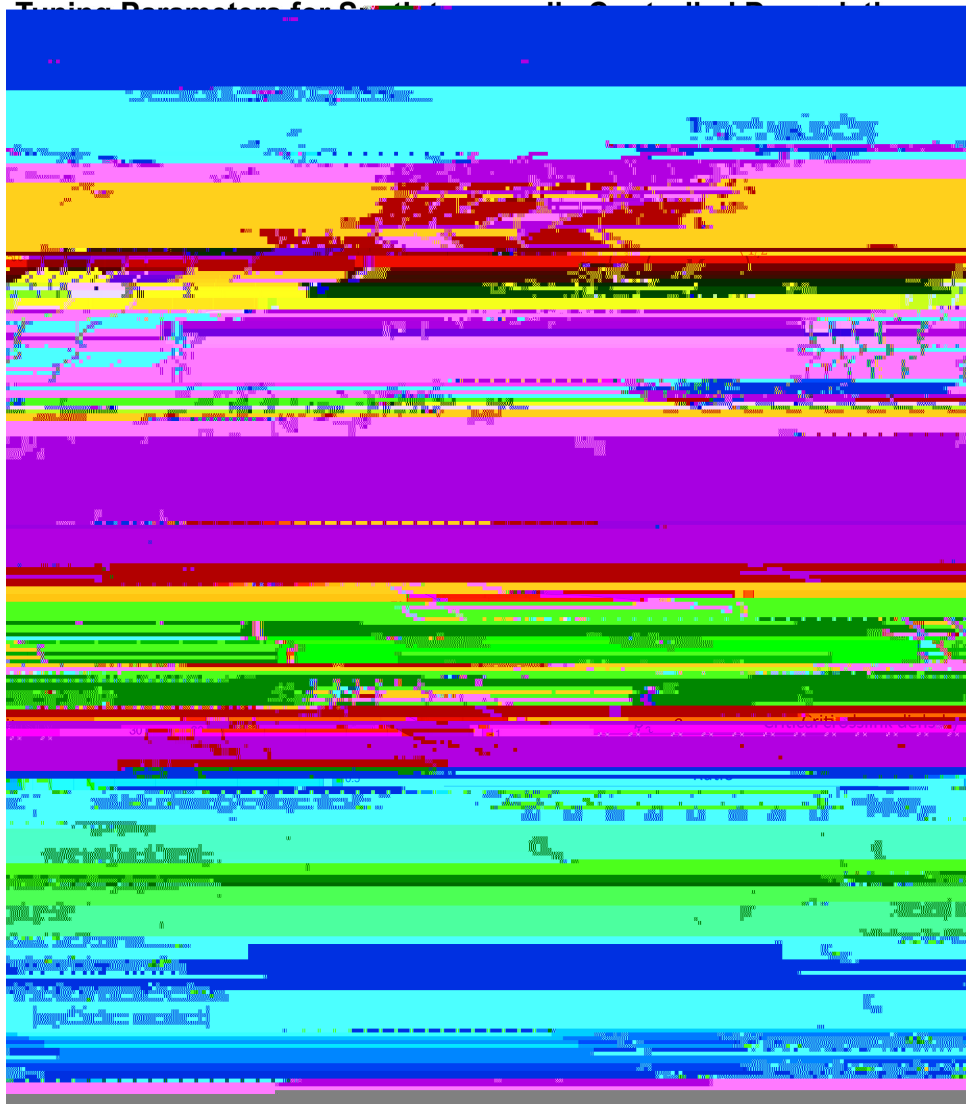


Figure 3. (a) Hydrogel fluorescence images showing the degradation of the hydrogel over time. The images show a central region of high fluorescence (red) surrounded by a lower fluorescence region (blue). The fluorescence intensity decreases over time, indicating degradation. (b) Compressive modulus of the hydrogel over time. The modulus decreases over time, indicating degradation. (c) Hydrogel wet weights over time. The wet weights are maintained over time, indicating that the degradation is primarily due to the loss of crosslinks rather than the loss of material. Parameters: $\alpha = 0.1$, $K_1 = 10 \times 10^6$ L mol⁻¹ s⁻¹, $K_2 = 10^4$ L mol⁻¹ s⁻¹, $K_3 = 10^4$ L mol⁻¹ s⁻¹, $K_4 = 10^4$ L mol⁻¹ s⁻¹, $K_5 = 10^4$ L mol⁻¹ s⁻¹, $K_6 = 10^4$ L mol⁻¹ s⁻¹, $K_7 = 10^4$ L mol⁻¹ s⁻¹, $K_8 = 10^4$ L mol⁻¹ s⁻¹, $K_9 = 10^4$ L mol⁻¹ s⁻¹, $K_{10} = 10^4$ L mol⁻¹ s⁻¹.

(Figure S5, Supporting Information). This release profile, as a degradation appeared to be restricted more locally in the region function of time, was input into the computational model to immediately surrounding the cell-mimetic. This observation is demonstrate the model's capability of incorporating complex supported by the following results: (a) the hydrogel fluorescence enzyme release profiles. Hydrogels were encapsulated with was largely maintained over time, but the size of the non- either collagenase-loaded microparticles or BSA-loaded micro-cent regions (originally correlating to the microspheres, which particles and the spatiotemporal degradation behavior and exhibited a distribution of sizes) increased statistically with time macroscopic properties were evaluated over time. In the low (Figure 2Cii,iii), (b) the compressive modulus decreased over crosslinked hydrogel, bulk degradation was evident by a rapid time, but the change was gradual (Figure 2Civ), and (c) hydrogel and overall decrease in hydrogel fluorescence (Figure 2Bi,ii). wet weights were maintained over time (Figure S6, Sup- Further, the compressive modulus (Figure 2Biii) decreased expo- porting Information). Simulations showed similar results with nentially while the hydrogel wet weights (Figure S6, Supporting a relatively sharp boundary surrounding the cell-mimetic and a Information) increased over time, consistent with the occurrence modulus that gradually decreased over time (Figure 2Dv,vi). In of bulk degradation. Simulations showed similar findings with addition, dual labeling of the hydrogel and enzyme qualitatively respect to a diffuse boundary surrounding the cell-mimetic and showed the spatiotemporal distribution of the hydrogel and a rapid loss in the compressive modulus of the bulk hydrogel enzyme over time, further supporting the above observations (Figure 2Biv,v). On the contrary in the high crosslink hydrogel, (Figure S7, Supporting Information).



Supporting Information

Supporting Information for this article is available as a supplementary PDF file, accessible from the article page on the journal website at www.advhealthmat.de.

Acknowledgements

This work was supported by the Deutsche Forschungsgemeinschaft (DFG) under the Special Collaborative Program SFB 101/0-1.

Received: 10/10/2015
 Accepted: 11/10/2015
 Published online: 12/10/2015

1. L. Wang, F. P. O. J. de Groot, J. A. J. van't Hof-Grootenboer, Nat. Biotechnol. 2003, 21, 13.

2. J. Wang, F. P. O. J. de Groot, J. A. J. van't Hof-Grootenboer, FASEB J 2011, 25, 13.

3. J. Wang, F. P. O. J. de Groot, J. A. J. van't Hof-Grootenboer, Adv. Healthcare Mater 2013, 2, 13.

4. J. Wang, F. P. O. J. de Groot, J. A. J. van't Hof-Grootenboer, Proc. Natl. Acad. Sci. USA 2015, 112, 13.

5. J. Wang, F. P. O. J. de Groot, J. A. J. van't Hof-Grootenboer, Adv. Healthcare Mater 2015, 4, 20.

6. J. Wang, F. P. O. J. de Groot, J. A. J. van't Hof-Grootenboer, Biomater. Sci 2014, 2, 102.

7. J. Wang, F. P. O. J. de Groot, J. A. J. van't Hof-Grootenboer, Annual Review of Cell and Developmental Biology, 26 (2010), 2010, 13.

8. J. Wang, F. P. O. J. de Groot, J. A. J. van't Hof-Grootenboer, Adv. Drug Delivery. Rev 2007, 59, 172.

9. J. Wang, F. P. O. J. de Groot, J. A. J. van't Hof-Grootenboer, Cancer Cell 2005, 7, 13.